Photochemical Properties of Mono-, Tri-, Penta-Cationic Antimony(V) Metalloporphyrin Derivatives on Clay Layer Surface.

ARTICLE *in* THE JOURNAL OF PHYSICAL CHEMISTRY A · JULY 2013

Impact Factor: 2.69 · DOI: 10.1021/jp405767s · Source: PubMed

3 AUTHORS, INCLUDING:

Shinsuke Takagi
Tokyo Metropolitan University
86 PUBLICATIONS **1,492** CITATIONS

THE JOURNAL OF PHYSICAL CHEMISTRY A

Article

pubs.acs.org/JPCA

Photochemical Properties of Mono-, Tri-, and Penta-Cationic Antimony(V) Metalloporphyrin Derivatives on a Clay Layer Surface

Takamasa Tsukamoto,[†] Tetsuya Shimada,[†] and Shinsuke Takagi*[,†,‡]

[†]Department of Applied Chemistry, Graduate Course of Urban Environmental Sciences, Tokyo Metropolitan University, Minami-ohsawa 1-1, Hachiohji, Tokyo 192-0397 Japan

[‡]PRESTO (Precursory Research for Embryonic Science and Technology), Japan Science and Technology Agency, 4-1-8 Honcho Kawaguchi, Saitama, Japan

Supporting Information

ABSTRACT: Three types of mono-, tri-, and penta-cationic antimony(V) porphyrin derivatives ($Sb^{V}Pors$) were synthesized, and their photochemical properties on the anionic clay were systematically investigated. $Sb^{V}Por$ derivatives are dihydroxo(5,10,15,20-tetraphenylporphyrinato)antimony(V) chloride ($[Sb^{V}(TPP)(OH)_2]^{+}Cl^{-}$), dihydroxo[5,10-diphenyl-15,20-di(*N*-methyl-pyridinium-4-yl)-porphyrinato]antimony(V) trichloride ($[Sb^{V}(DMPyP)(OH)_2]^{3+}3Cl^{-}$), and dihydroxo[5,10,15,20-tetrakis(*N*-methyl-pyridinium-4-yl)-porphyrinato]antimony(V) pentachloride ($[Sb^{V}(TMPyP)(OH)_2]^{5+}5Cl^{-}$). The photochemical behaviors of three cationic $Sb^{V}Pors$ with and without clay were examined in aqueous solution. For all $Sb^{V}Por$, aggregation behaviors were not observed in the clay complexes even at high density adsorption conditions. The transition probabilities and fluorescence quantum yields of $Sb^{V}Por$ showed a tendency to be increased by the complex formation with clay. The less cationic $Sb^{V}Por$/clay complex showed the larger fluorescence quantum yield. The more cationic $Sb^{V}Por$/clay complex showed the longer fluorescence lifetime. These effects of complex formation with clay on the photochemical properties of $Sb^{V}Pors$ were discussed using the molecular potential energy curves of the porphyrin ground state and excited state. It is concluded that two types of effects work in the $Sb^{V}Por$/clay system: effect i (structure resembling effect) is that the most stable structure becomes relatively similar between the ground and excited states, mainly by hydrophobic interactions between the porphyrin molecule and the clay surface, and effect ii (structure fixing effect) is that sharpened potential energy curves of clay complexes can lead to the increase of activation energy for the internal conversion from excited state to a high vibration level of ground state, mainly by electrostatic interactions between cationic porphyrin and anionic clay. Like this, the unique effects of the clay surface on the photochemical behavior of dyes were observed and the mechanisms were rationally discussed.

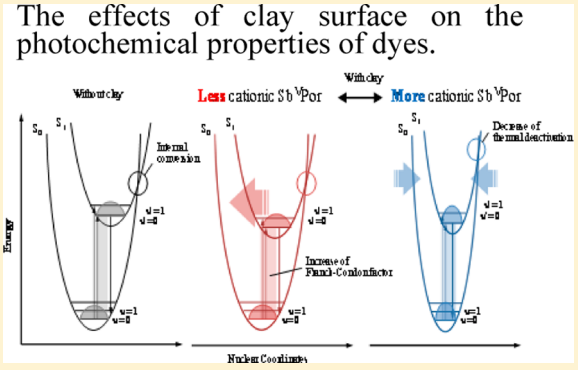

INTRODUCTION

Complexes between dye molecules and inorganic host materials such as clay minerals, zeolite, silica, or alumina provide photochemical functions and versatility[1−22] as a molecular orientation or aggregation controlling field,[1,3,7,10,15,17] or photochemical reaction field.[4,9,11] Generally, the adsorbed dyes have a tendency to aggregate on or in such inorganic host materials.[4,23] An aggregation such as H-aggregation in general decreases the excited-state lifetimes of dyes drastically and is not favored for intermolecular photochemical reactions. However, the control of aggregation behavior of dyes on the inorganic surface has been considered difficult, in the past. Recently, we reported that +4-charged porphyrin molecules having pyridinium as a *meso*-substituent adsorb on nanosheets of saponite without aggregation even at high dye loadings.[24−29] These interesting behaviors were rationalized by a size-matching of the distances between the cationic sites in porphyrin molecules and those between the anionic sites on the clay surface. We named this effect as "inter-charge distance matching effect" or "size-matching effect".[7,27−29] This effect can strengthen the host−guest interaction enough to avoid the aggregation due to guest−guest interaction.

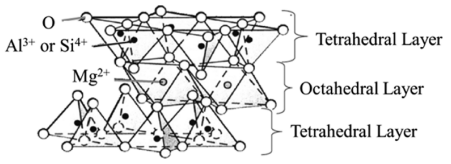

Figure 1. The structure of synthetic saponite, $[(Si_{7.2}Al_{0.8})(Mg_{5.97}Al_{0.03})O_{20}(OH)_4]^{-0.77}$.

Clay minerals[1−6,30−33] are interesting multilayered inorganic compounds as host materials of organic−inorganic complexes.[1−6,30,31,33,34] Some clay minerals such as saponite have the cation exchange capacity (CEC) originated from the negatively charged structure of nanosheets. The structure of typical clay (synthetic saponite) is shown in Figure 1. Its stoichiometric formula is $[(Si_{7.2}Al_{0.8})(Mg_{5.97}Al_{0.03})O_{20}(OH)_4]^{-0.77}$.

Received: June 11, 2013
Revised: July 22, 2013
Published: July 25, 2013

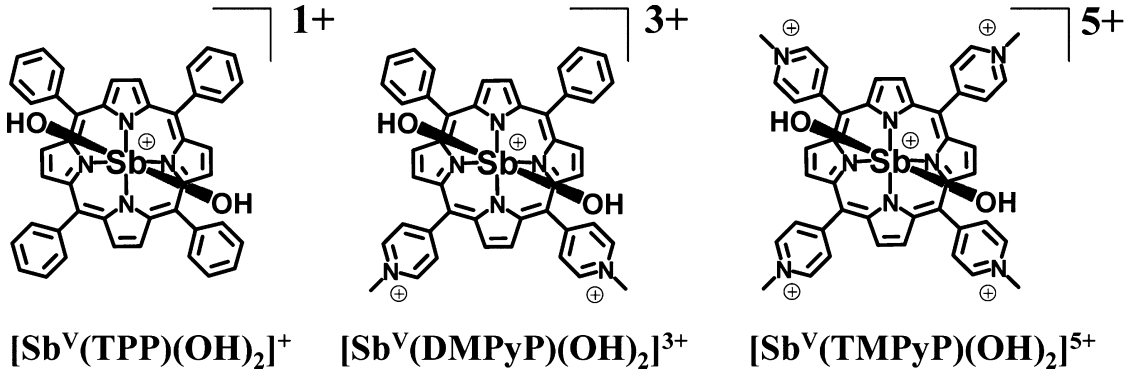

Figure 2. Structures of dihydroxo(5,10,15,20-tetraphenylporphyrinato)antimony(V) ($[Sb^{V}(TPP)(OH)_2]^+$), dihydroxo[5,10-diphenyl-15,20-di(*N*-methyl-pyridinium-4-yl)porphyrinato]antimony(V) ($[Sb^{V}(DMPyP)(OH)_2]^{3+}$), and dihydroxo[5,10,15,20-tetrakis(*N*-methyl-pyridinium-4-yl)-porphyrinato]-antimony(V) ($[Sb^{V}(TMPyP)(OH)_2]^{5+}$).

$(Na_{0.49}Mg_{0.14})^{+0.77}$, the theoretical surface area is 750 m^2 g^{-1}, and the cationic exchange capacity (CEC) is 99.7 mequiv/100 g. The average area per anionic site is calculated to be 1.25 nm^2, and the average distance between anionic sites on the clay surface is estimated to be 1.2 nm, on the basis of the assumption of a hexagonal array.[7] Since the aqueous solution of saponite is transparent in the UV−visible range when the particle size exfoliated in water is small (<200 nm), they are suitable for optical measurement and constructing the photochemical reaction system.

The unique photochemical behaviors of the dyes in the clay complex have been reported. The absorption maxima of porphyrin are shifted to longer wavelength by the complex formation with clay.[7,19,23,29] The mechanism of the unique absorption spectral shifts of porphyrin molecules upon adsorption on the clay surface is experimentally confirmed to be the flattening of the *meso*-substituent with respect to the plane of the porphyrin ring.[29] Although the fluorescence enhancement is observed for some dye molecules by the complex formation with clay,[35−37] the fluorescence of dye molecules tends to be quenched by the self-quenching process on the clay surface. This behavior is also not favored for the construction of efficient photochemical reaction systems. We reported that "size-matching" porphyrins tend not to suffer self-fluorescence quenching even at 100% adsorption versus the CEC of the clay.[38,39]

In this work, we synthesized multicationic antimony(V) porphyrins that are expected to adsorb well and provide photofunctionality on the anionic saponite surface. Photochemical behaviors of three types of +1, +3, and +5 charged antimony(V) porphyrin derivatives (Sb^{V}Pors) in the clay complex were systematically investigated. Sb^{V}Pors are dihydroxo (5,10,15,20-tetraphenylporphyrinato)antimony(V) chloride ($[Sb^{V}(TPP)(OH)_2]Cl$), dihydroxo [5,10-diphenyl-15,20-di(*N*-methyl-pyridinium-4-yl)porphyrinato]antimony(V) trichloride ($[Sb^{V}(DMPyP)(OH)_2]Cl_3$), and dihydroxo[5,10,15,20-tetrakis(*N*-methyl-pyridinium-4-yl)porphyrinato]antimony(V) pentachloride ($[Sb^{V}(TMPyP)(OH)_2]Cl_5$) (Figure 2). The adsorption behavior and photochemical properties of these cationic Sb^{V}Pors on an anionic clay surface were investigated by UV−visible absorption, steady, and time-resolved fluorescence spectroscopy by controlling the loading levels of cationic Sb^{V}Por versus the CEC of the clay. The complexes were examined in water in which the saponite clay sheet is exfoliated as a single nanosheet.

Porphyrin and metalloporphyrin generally have photoredox ability at their excited states.[40] Especially tetraphenylantimony(V) complexes (Sb^{V}TPP) have been reported to be important as a sensitizer or photocatalyst.[41−49] The Sb^{V}porphyrin/clay complex could be used as a photocatalyst of the photochemical oxygenation reaction. Sb^{V}TPP complexes are +1 charged cationic porphyrin where the positive charge delocalizes in a π-electron system of a porphyrin ring and two axial ligands.[50,51] Although the adsorption behaviors of multicationic free-based porphyrins having pyridinium as a *meso*-substitutent on the clay surface were well reported,[7,24−29,38,39] there were only a few reports on mono-cationic Sb^{V}TPP complexes on the clay surface.[45,51−53] Especially, the photochemical behaviors of porphyrins having both cationic central metal and cationic peripheral substituents on the inorganic surface have not been reported as far as we know. In this paper, the effect of both cationic central metal and cationic peripheral substituents on the adsorption behavior onto the clay surface and their photochemical behaviors were investigated.

EXPERIMENTAL SECTION

Materials. Clay minerals (saponite): Sumecton SA was received from Kunimine Industries Co., Ltd. Dihydroxo(5,10,15,20-tetraphenylporphyrinato)antimony(V) chloride ($[Sb^{V}(TPP)(OH)_2]Cl$, denoted as Sb^{V}TPP), dihydroxo[5,10-diphenyl-15,20-di(*N*-methyl-pyridinium-4-yl)porphyrinato]antimony(V) trichloride ($[Sb^{V}(DMPyP)(OH)_2]Cl_3$, denoted as Sb^{V}DMPyP), and dihydroxo[5,10,15,20-tetrakis(*N*-methyl-pyridinium-4-yl)porphyrinato]antimony(V) pentachloride ($[Sb^{V}(TMPyP)(OH)_2]Cl_5$, denoted as Sb^{V}TMPyP) were synthesized as described in the Supporting Information.

UV−visible absorption spectra were obtained on a Shimadzu UV-3150 spectrophotometer. Emission spectra were recorded on a Jasco FP-6600 spectrofluorometer. Time-resolved fluorescence signals were measured by a Hamamatsu Photonics C4780 detector system based on a streak camera. A Nd^{3+} YAG laser with an OPG (EKSPLA PL2210JE + PG-432, fwhm 25 ps, 1 kHz) was used for excitation. The orientation angles of the porphyrins were observed by polarized absorption spectroscopy by the use of an interface spectrometer equipped with a quartz waveguide system (System Instruments, SIS-50BS).[54,55]

Sample Preparation for Absorption Spectra. Exfoliated porphyrin/saponite complexes were prepared by mixing an aqueous clay dispersion and the respective cationic porphyrin aqueous solutions under stirring. The concentration of clay for the Lambert−Beer plot was 1.0×10^{-6}, 3.0×10^{-6}, and 5.0×10^{-6} equiv L^{-1} for Sb^{V}TPP, Sb^{V}DMPyP, and Sb^{V}TMPyP, respectively. The loading levels of cationic porphyrins versus the CEC of the clay in the complexes were controlled by varying the concentrations of porphyrins.

Sample Preparation for Waveguide Dichroic Absorption Spectra. The dichroic spectra on the waveguide were measured according to the literature.[54,55] The aqueous dispersion of the

clay was cast onto the quartz waveguide, and the waveguide was dried under air. The area on the quartz waveguide covered with the clay was around 1.5 cm^2. The aqueous porphyrin was put on the quartz waveguide covered with the clay. The porphyrin loadings were set at 2.0×10^{-2} molecules nm^{-2}. The tilt angle of the porphyrins against the clay surface was determined by a quantitative analysis of the p/s ratio of the absorbance including a theoretical derivation of the dichroic absorption.[54,55]

Sample Preparation for Fluorescence Spectra. The preparation method for the porphyrin/saponite complex is the same to that for absorption spectra. The concentrations of all porphyrins were 1.0×10^{-7} M. The loading levels of cationic porphyrins versus the CEC of the clay in the complexes were controlled by varying the concentration of clay. The fluorescence quantum yields of porphyrins were determined using $[H_2TMPyP]Cl_4$ as the standard ($\Phi_f = 0.050$).[56]

Sample Preparation for Time-Resolved Fluorescence Spectra. The preparation method for the porphyrin/saponite complexes is the same as that for absorption spectra. The porphyrin loadings were set at 5.0×10^{-4} molecules nm^{-2}.

RESULTS AND DISCUSSION

Absorption Spectral Behavior of Sb^VPors with and without Clay. The aqueous clay dispersion was essentially transparent in the UV−visible region under the present experimental conditions. UV−visible absorption spectra of the porphyrins in water and adsorbed on the saponite surface were observed. The absorption spectra of Sb^VTPP, Sb^VDMPyP, and Sb^VTMPyP with and without clay are shown in Figure 3.

All porphyrins showed the spectral shift to longer wavelengths upon the complex formation with clay. These red shifts of the porphyrin upon adsorption on the clay surface are known to be mainly induced by the coplanarization of *meso*-substituents with respect to the porphyrin rings.[7,19,22,29] As described later, the aggregation of Sb^VPors, that can induce the spectral shift, does not take place under the present conditions. Thus, the degrees of red shifts are useful to discuss the adsorption conditions of molecules on the clay surface, such as their degree of molecular flattening. The values of spectral shifts ($\Delta\lambda_{max}$) at the Soret band were 14 nm (0.097 eV), 13 nm (0.090 eV), and 10 nm (0.071 eV) for Sb^VTPP, Sb^VDMPyP, and Sb^VTMPyP, respectively. There was almost no difference between $\Delta\lambda_{max}$ of all Sb^VPors. This result suggests that structures of Sb^VPors adsorbed on the clay surface are flattened compared to those in bulk solution in a similar way among Sb^VPors. The orientation angles of the porphyrin plane with respect to the clay surface were estimated by dichroic measurements on the quartz waveguide using polarized visible-light-attenuated total reflectance spectroscopy (PV-ATR).[54,55] The absorbance with s-polarized light was much larger than that with p-polarized light for the Sb^VTPP/clay complex (Figure S1, Supporting Information). The orientation angles were calculated to be 21, 20, and 11° for Sb^VTPP, Sb^VDMPyP, and Sb^VTMPyP, respectively. It is confirmed that all Sb^VPors adsorb on the clay surface with nearly parallel orientation that can induce the coplanarization of *meso*-substituents with respect to the porphyrin rings. Interestingly, the values of integrals of the extinction coefficients ($\int\varepsilon_Q$) in Q-band wavenumber range between with and without clay were distinctly different (Table 1). For all porphyrins, $\int\varepsilon_Q$ values of porphyrins on the clay surface increased about 1.6 times compared with those in the bulk solution. These results indicate that the transition probabilities of porphyrins increased by the complex formation with clay. The increase of the transition probability of porphyrin would be due to the increase of Franck−Condon factor on the clay surface. The effect of complex formation with clay on the potential surfaces of the ground and excited states of porphyrin is described later.

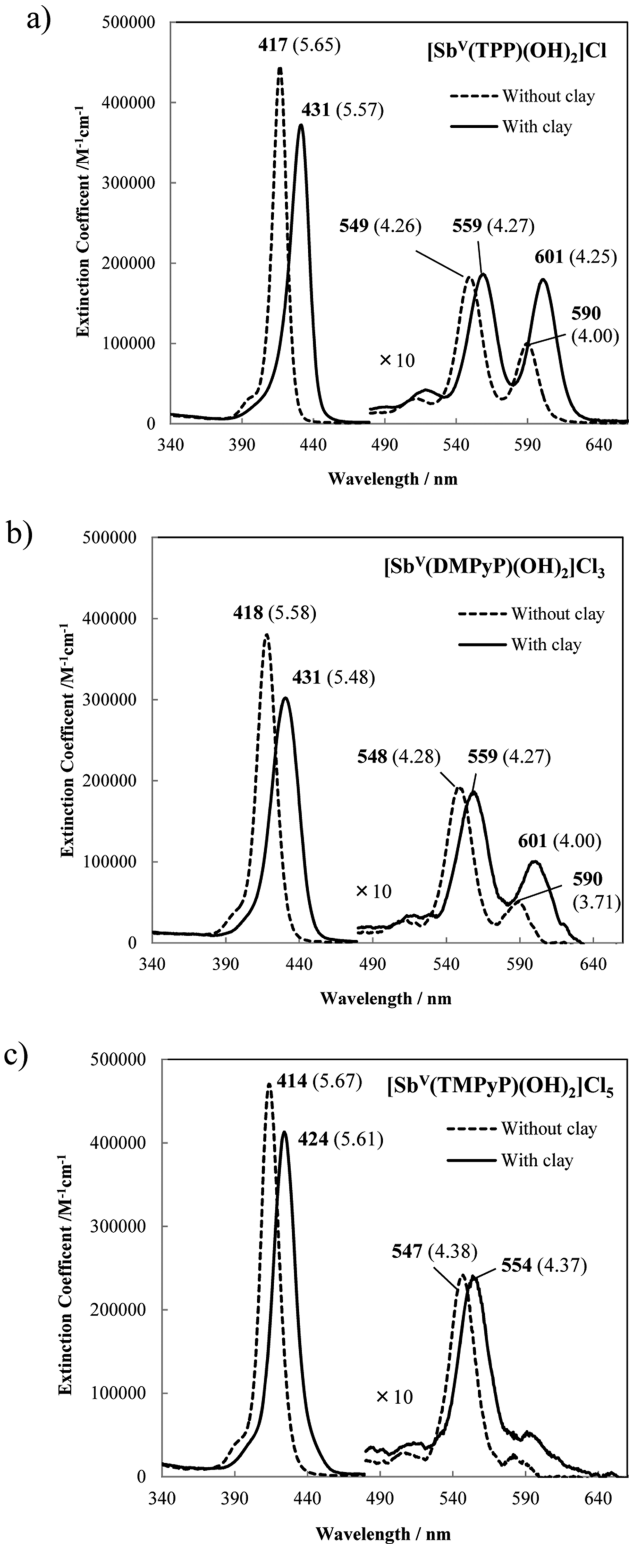

Figure 3. Absorption spectra of (a) Sb^VTPP, (b) Sb^VDMPyP, and (c) Sb^VTMPyP with and without clay in water. Absorption maxima values (λ_{max}/nm) and the extinction coefficients (log ε_{max}) are shown. [Saponite] = 6.0×10^{-5} equiv L^{-1} (the loading levels of porphyrins are 10% versus the CEC of the clay).

dx.doi.org/10.1021/jp405767s | J. Phys. Chem. A 2013, 117, 7823−7832

Table 1. The Values of Integrals of the Extinction Coefficients ($\int \varepsilon_Q$) of Sb^VPors with and without Clay in Water in the Q-Band Wavenumber Range[a]

compound	integral of the extinction coefficient ($\times 10^5$ M^{-1} cm^{-2}) $\int \varepsilon_Q{}^W$	$\int \varepsilon_Q{}^C$	$\int \varepsilon_Q{}^C / \int \varepsilon_Q{}^W$
$[Sb^V(TPP)(OH)_2]Cl$	0.915	1.43	1.56
$[Sb^V(DMPyP)(OH)_2]Cl_3$	0.701	1.10	1.57
$[Sb^V(TMPyP)(OH)_2]Cl_5$	0.737	1.18	1.60

[a]The integral range is 14500−20400 cm^{-1} (490−690 nm). $\int \varepsilon_Q{}^W$ and $\int \varepsilon_Q{}^C$ are the $\int \varepsilon_Q$ of Sb^VPor without clay and with clay.

It should be noted that there are differences of the Q-band shapes of Sb^VPors between with and without clay. On the clay surface, the ratios of the extinction coefficients of the α (Q(0,0)) and β (Q(1,0)) bands ($\varepsilon_\alpha/\varepsilon_\beta$) on the clay surface increased about 2 times compared with those in the bulk solution. The Q(n,0) band is a transition from the lowest vibration level ($\nu = 0$) of the ground state (S_0) to the high vibrational level ($\nu' = n$) of the excited state (S_1) for porphyrins. These results indicate that the transition probabilities of the α and β bands changed, due to the change of each Franck−Condon factor. It is suggested that the molecular structures of the ground and excited states of porphyrin become similar by the complex formation with clay. This speculation coincides well with the discussions described later.

Adsorption Behavior of Sb^VPors on the Clay Surface. The concentration effects of Sb^VPor on the absorption spectra were examined as shown in Figure 4. For all Sb^VPors, the absorption increased without any shape change in the early stage; then, new species appeared at a certain loading level as the Sb^VPor loading level increased. The new species are aggregates and/or nonadsorbed species of Sb^VPor. In the case of Sb^VTPP (Figure 4, **1a**, **1b**), above 20% versus the CEC adsorption, the spectrum of aggregated Sb^VTPP (indicated as II) was newly superimposed on the spectra. Here, an aggregate is defined as the state where the transition dipole moments of adjacent Sb^VPor molecules interact with each other and the absorption spectra are altered. Above 90% loading, the spectrum of nonadsorbed Sb^VTPP in the bulk solution was additionally observed (not shown). Interestingly, the linearity of the Lambert−Beer plot was also kept in the aggregation region. In the case of Sb^VDMPyP (Figure 4, **2a**, **2b**), above 75% versus the CEC, nonadsorbed Sb^VDMPyP in bulk solution newly appeared and aggregated Sb^VDMPyP was not observed at any loading level. Sedimentation of the porphyrin/clay complex due to neutralizing clay anionic charge by Sb^VDMPyP at around 100% versus CEC loading was observed. In the case of Sb^VTMPyP (Figure 4, **3a**, **3b**), above 80% versus CEC, nonadsorbed Sb^VTMPyP in bulk solution was newly superimposed on the spectra. Like this, judging from the spectral shape and the linearity of the Lambert−Beer plot (Figure 4, **1**−**3b**), the maximum adsorption amounts of Sb^VPors without aggregation were determined to be 20, 75, and 80% versus CEC for Sb^VTPP, Sb^VDMPyP, and Sb^VTMPyP, respectively.

Using % versus CEC of clay as a unit is not convenient to discuss the adsorption structure of Sb^VPors on the clay surface, since the intramolecular cation numbers are different in each Sb^VPor. Thus, the adsorption densities and the calculated average intermolecular distances of porphyrins at maximum adsorption without aggregation on the clay surface are shown and summarized in addition to % versus CEC in Table 2. According to the data in Table 2, the speculated adsorption structures of Sb^VPors at maximum adsorption condition on the basis of hexagonal array are shown in Figure 5.

As described in the Introduction section, organic molecules easily form their aggregates on the inorganic surface even at the low density conditions. Compared to this, the adsorption densities of all Sb^VPor where aggregation behaviors are not observed seem to be very high. If the deviation of center-to-center distances between Sb^VPor molecules was large, spectral changes due to aggregation for Sb^VPor molecules whose center-to-center distance is short would be observed. Thus, the deviation of average intermolecular distances should be small. According to the size-matching rule, nonaggregation behavior is reasonable for Sb^VDMPyP and Sb^VTMPyP. In the case of mono-cationic Sb^VTPP, other mechanisms suppressing the aggregation should be discussed. To form the aggregates, a standing orientation of porphyrin molecule on the clay surface would be favored. Sb^VTPP adsorbs the clay surface with parallel orientation due to the position of the cationic part and a hydrophobic interaction between the porphyrin aromatic ring and the clay surface. In the case of Sb^VTPP, the position of the cationic part is in the center of the molecule. At the present, we believe that such parallel orientation of molecule on the solid surface plays an important role in preventing the molecular aggregation.

Fluorescence Spectral Behavior of Sb^VPors with and without Clay. Fluorescence spectra of porphyrins in water and adsorbed on the saponite surface were observed. The fluorescence spectra of porphyrins with and without clay are shown in Figure 6. The loading levels of Sb^VPors were set at 10% versus CEC, where aggregation behavior was not observed.

In all porphyrins, red-shifts of the fluorescence maximum (λ_{em}) were observed and the shapes of the fluorescence spectra reflected the absorption spectra in each porphyrin with and without clay. The fluorescence quantum yields (Φ_f) are summarized in Table 3. $\Phi_f{}^W$ and $\Phi_f{}^C$ are the Φ_f of Sb^VPor with clay and without clay, respectively. The value of Φ_f for Sb^VPor showed a tendency to be enhanced by the complex formation with clay, compared to that without clay. As the number of cationic parts in Sb^VPor decreased, the value of Φ^C/Φ^W increased. To discuss the detail of photochemical behavior of porphyrins on the clay surface, time-resolved fluorescence spectra for each porphyrin with and without clay were measured to obtain the excited lifetime by using the picosecond fluorescence measurement system. As shown in Figure 7, all decay curves for porphyrins with and without clay can be analyzed as a single exponential decay, and the fluorescence lifetimes (τ) were obtained. The result indicates that fluorescence is emitted from porphyrins as a monomer and they uniformly adsorb on the clay nanosheet. It should be noted that such a simple decay curve is hardly obtained in usual dye−inorganic hybrids. The values of τ^W, τ^C, and τ^C/τ^W are summarized in Table 3. As the cationic valence in Sb^VPor increased, the number of cationic parts of τ^C/τ^W increased.

The radiative deactivation rate constants for fluorescence (k_f) and nonradiative deactivation rate constants (k_{nr}) were calculated by using values of fluorescence quantum yields (Φ_f) and fluorescence lifetimes (τ) according to eqs 1 and 2, and are shown in Table 4. The ratios of k^C and k^W are shown in Table 4 to discuss effects of clay in detail.

$$k_f = \frac{\Phi_f}{\tau} \quad (1)$$

$$k_{nr} = \frac{(1 - \Phi_f)}{\tau} \quad (2)$$

dx.doi.org/10.1021/jp405767s | J. Phys. Chem. A 2013, 117, 7823−7832

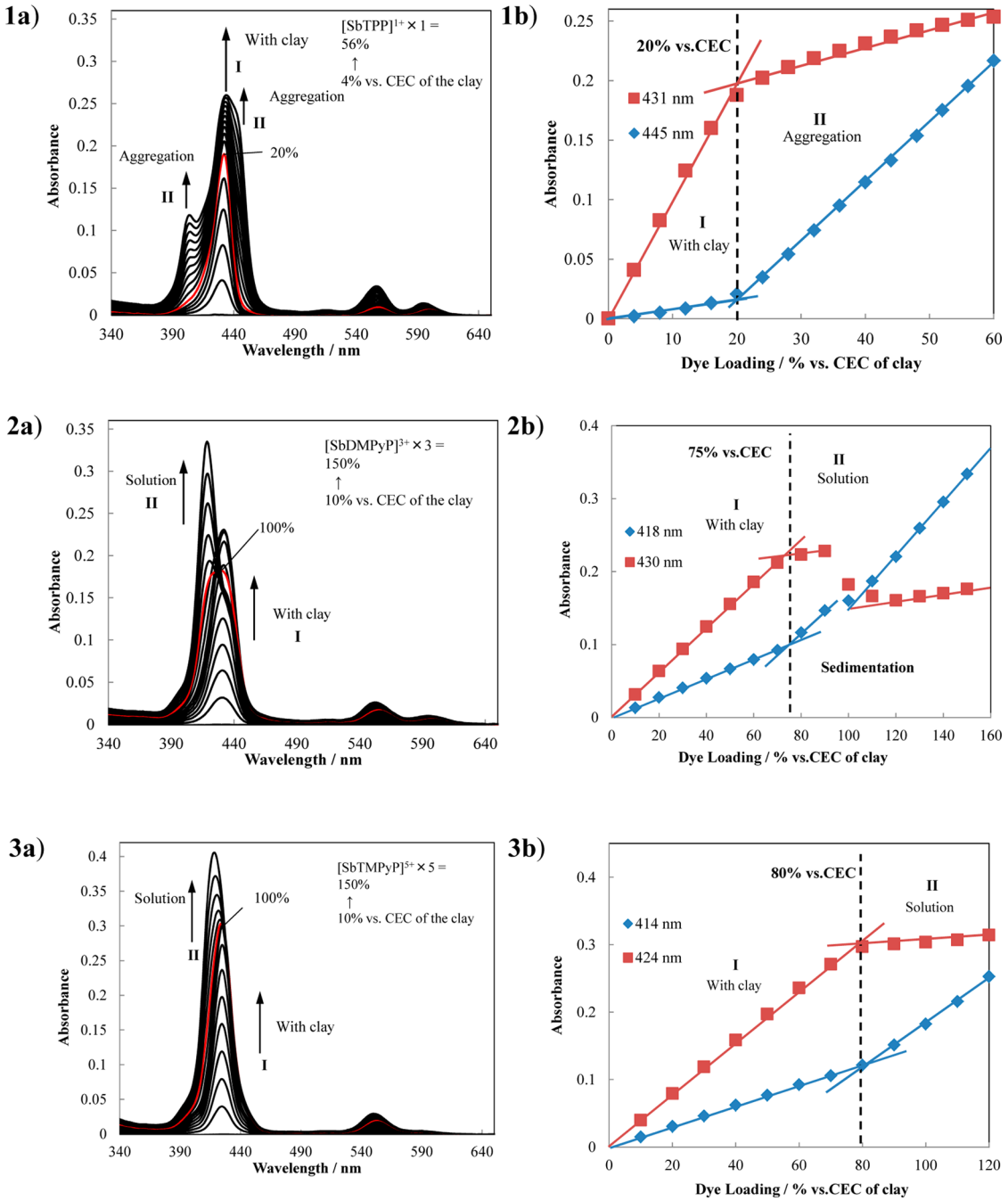

Figure 4. Absorption spectra of Sb^{V}Por/saponite complexes at various Sb^{V}Por concentrations (**1a** for Sb^{V}TPP, **2a** for Sb^{V}DMPyP, and **3a** for Sb^{V}TMPyP) and Lambert–Beer plots for Sb^{V}Por/saponite complexes at 431 and 445 nm up to 60% vs CEC ([saponite] = 2.5×10^{-6} equiv L^{-1}) for Sb^{V}TPP (**1b**), at 418 and 430 nm up to 150% vs CEC ([saponite] = 3.0×10^{-6} equiv L^{-1}) for Sb^{V}DMPyP (**2b**), and at 414 and 424 nm up to 120% vs CEC ([saponite] = 5.0×10^{-6} equiv L^{-1}) for Sb^{V}TMPyP (**3b**) in aqueous transparent solution.

Table 2. The Loading Levels, the Adsorption Densities, and the Average Distances between Porphyrin Molecules at Maximum Adsorption Conditions without Aggregation[a]

compound	loading level (% vs CEC)	aggregation over maximum adsorption	adsorption density (molecules nm^{-2})	average intermolecular distance (nm)
$[Sb^{V}(TPP)(OH)_2]Cl$	20	yes	0.16	2.7
$[Sb^{V}(DMPyP)(OH)_2]Cl_3$	75	no	0.20	2.4
$[Sb^{V}(TMPyP)(OH)_2]Cl_5$	80	no	0.13	3.0

[a]The average intermolecular distance is the center to center of porphyrin molecules.

For less cationic Sb^{V}Por, both k_f^C/k_f^W and k_{nr}^C/k_{nr}^W increased. The effects of complex formation with clay on the photochemical properties of dyes can be discussed by using potential energy curves of the ground and excited states of dye

dx.doi.org/10.1021/jp405767s | J. Phys. Chem. A 2013, 117, 7823−7832

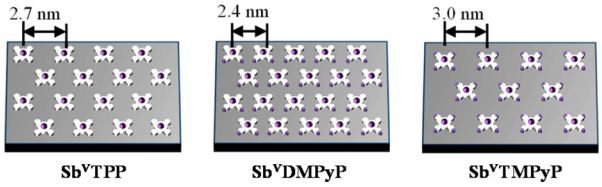

Figure 5. The schematic representation of the maximum adsorption structure of Sb^{V}Pors on the clay surface under a nonaggregation condition. The loading levels of porphyrins are 20, 75, and 80% vs CEC for Sb^{V}TPP, Sb^{V}DMPyP, and Sb^{V}TMPyP, respectively.

molecule.[35] It has been reported that there are two types of effects: (i) the most stable structure becomes relatively similar between the ground and excited states (effect i (structure resembling effect)) and (ii) the potential energy curves are relatively sensitive against the nuclear coordinates (effect ii (structure fixing effect)) (Figure 8). Effect i induces the increase of k_f values because of the large Franck−Condon factor due to the similarity of molecular structure between the ground and excited states, and effect ii induces the decrease of k_{nr} values because the potential energy curves of the ground and excited states cross at the high vibration state of the excited state's potential energy curve that can be rationalized by the fact that the molecular structural changes are suppressed and the potential energy curves on the clay surface become sharp.[35] On the basis of these effects, the present result is discussed. The major interaction between Sb^{V}Por molecules and the clay surface would be electrostatic and hydrophobic interactions.[27]

For less cationic Sb^{V}Por, larger k_f^{C}/k_f^{W} values were observed. This suggests that effect i is mainly working for less cationic Sb^{V}Por to make the structure of the excited state similar to that of the ground state, leading to a large Franck−Condon factor (Figure 8b). The absorption probabilities of all porphyrins on the clay surface were larger than that of bulk solution according

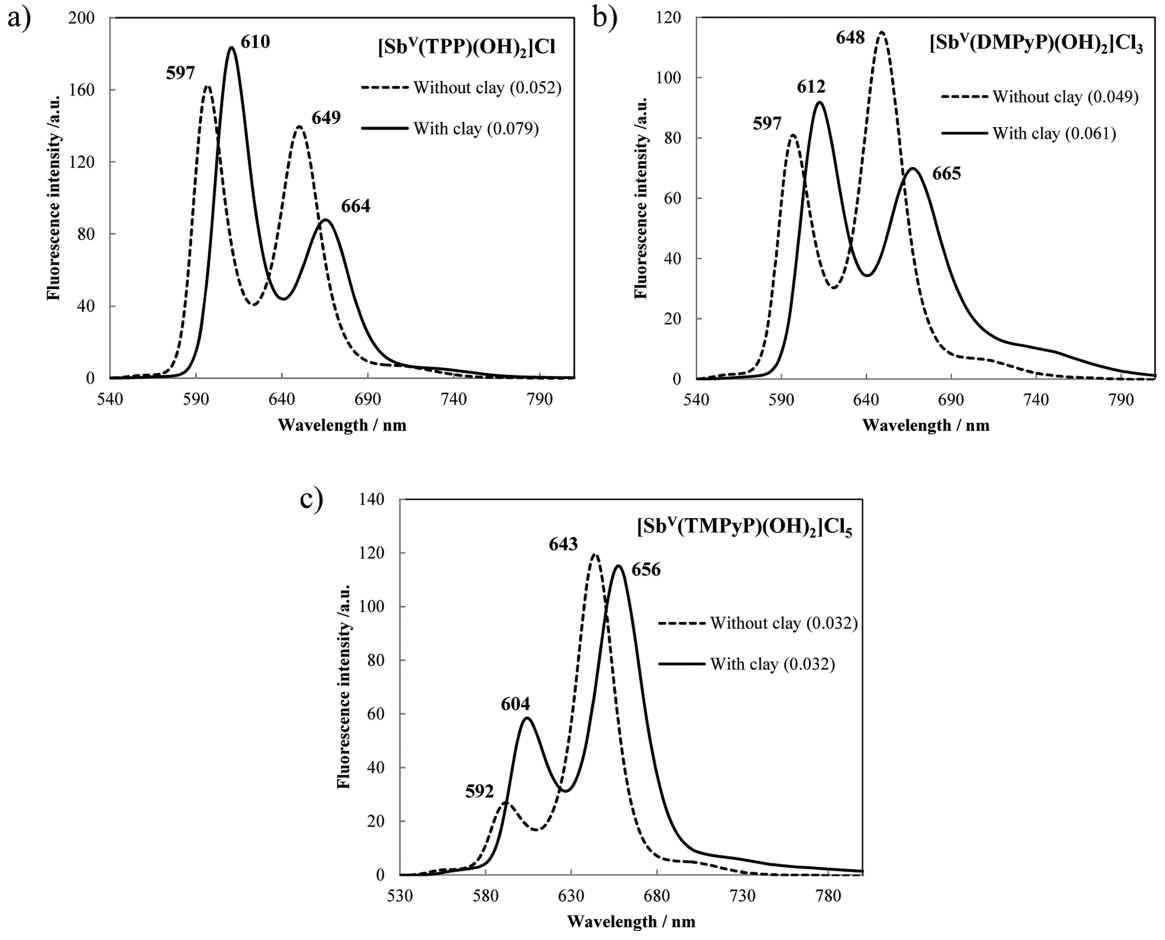

Figure 6. Fluorescence spectra and fluorescence peaks (λ_{em}/nm) excited at 431 and 417 nm, 431 and 418 nm, and 426 and 414 nm for (a) Sb^{V}TPP, (b) Sb^{V}DMPyP, and (c) Sb^{V}TMPyP with and without clay in water, respectively. The fluorescence quantum yields (Φ_f) are shown in the brackets. [Sb^{V}Por] = 1.0×10^{-7} M (the loading levels of porphyrins were 10% versus CEC of the clay).

Table 3. The Fluorescence Quantum Yields (Φ_f) and the Fluorescence Lifetimes (τ) of Sb^{V}Por with and without Clay in Water[a]

	fluorescence quantum yield			fluorescence lifetime		
compound	Φ_f^{W}	Φ_f^{C}	Φ_f^{C}/Φ_f^{W}	τ^{W} (ns)	τ^{C} (ns)	τ^{C}/τ^{W}
$[Sb^{V}(TPP)(OH)_2]Cl$	0.052	0.079	1.52	1.3	0.9	0.69
$[Sb^{V}(DMPyP)(OH)_2]Cl_3$	0.049	0.061	1.24	1.3	1.1	0.85
$[Sb^{V}(TMPyP)(OH)_2]Cl_5$	0.032	0.032	1.00	1.2	1.6	1.33

[a] Φ_f^{W} and Φ_f^{C} are the Φ_f of Sb^{V}Por without clay and with clay. τ^{W} and τ^{C} are the τ of Sb^{V}Por without clay and with clay.

dx.doi.org/10.1021/jp405767s | J. Phys. Chem. A 2013, 117, 7823−7832

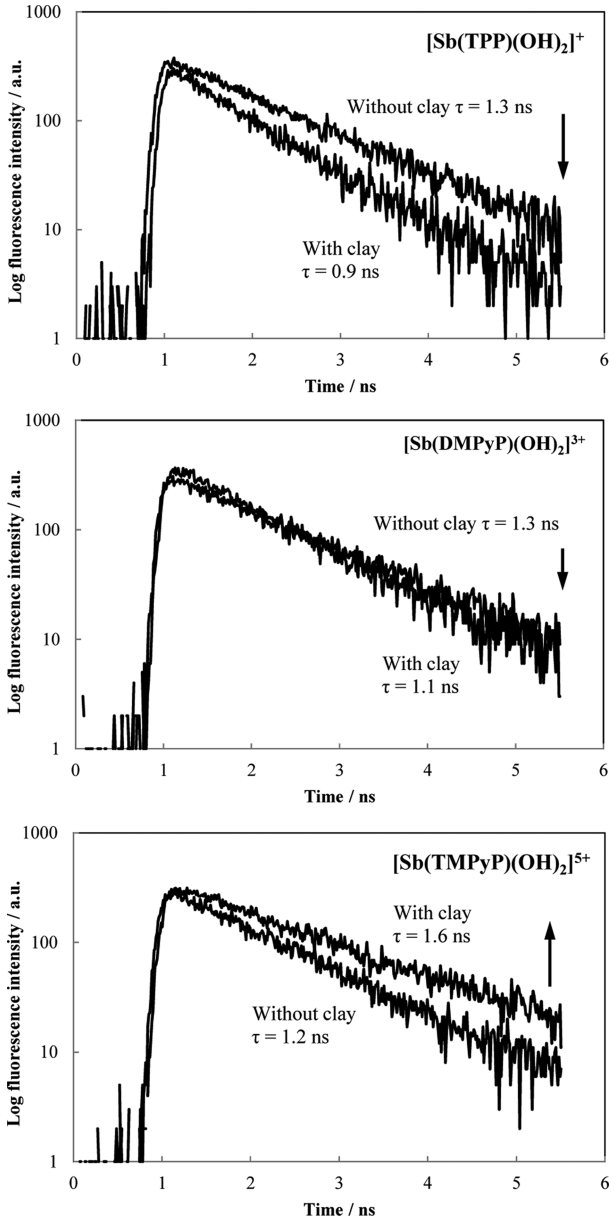

Figure 7. Fluorescence decay profile and fluorescence lifetimes (τ) of porphyrins excited with and without clay in water. The porphyrin loadings on the clay surface were 5×10^{-4} molecules nm^{-2}.

to the absorption spectra, as shown in Figure 3. This result indicates the increase of transition moment by the increase of Franck−Condon factor for all porphyrins. In addition, the increase of Q(0,0) absorptions and the decrease of Q(1,0) absorptions were observed for all porphyrins on the clay surface, as can be seen in Figure 3. Furthermore, the increase of relative intensities of Q(0,0) emissions to Q(0,1) emissions were observed for all porphyrins on the clay surface, as can be seen in Figure 6. This result also clearly indicates changes of transition moment by changes of Franck−Condon factor due to effect i (the structure resembling effect) for all porphyrins (Figure 8b). These results suggest that hydrophobic interaction between the clay surface and the porphyrin molecule is working for all Sb^{V}Pors.

For more cationic Sb^{V}Pors, smaller k_{nr}^{C}/k_{nr}^{W} values were observed. This result can be explained mainly by effect ii. For example, Sb^{V}TMPyP adsorbs on clay with five point electrostatic interactions, leading to the strong fixation of molecular structure. This fact corresponds to the sharp potential energy curves in the case of Sb^{V}TMPyP. Although the total effect depends on the balance of effects i and ii, sharpened potential energy curves can lead to the increase of activation energy for the internal conversion from the excited state to a high vibration level of the ground state, leading to a decrease of k_{nr} (Figure 8c). As a result, effect i is mainly working for less cationic Sb^{V}Por through hydrophobic interaction, and effect ii is mainly working for more cationic Sb^{V}Por through electrostatic interaction. It should be noticed that an electrostatic interaction works approximately with point to point as an enthalpy term thus can fix the molecular structure strongly. On the other hand, hydrophobic interaction works including water molecules and thus the structure fixing effect should be weak.

Self-Fluorescence Quenching Behaviors of Sb^{V}Por/Clay Complexes. The self-fluorescence quenching behaviors of the porphyrin/clay complexes were examined. In the present system, the aggregation is completely suppressed and the decomposition due to light irradiation does not occur judging from absorption spectra. Thus, the self-fluorescence quenching in this system is supposed to be induced by an electron transfer reaction between adjacent adsorbed molecules on the clay surface.[29] Fluorescence spectra of complexes for porphyrins at different loading levels are shown in Figure 9. The concentration of porphyrins was kept constant at 1.0×10^{-7} M to retain the same absorbance in all cases, and the loading level was controlled

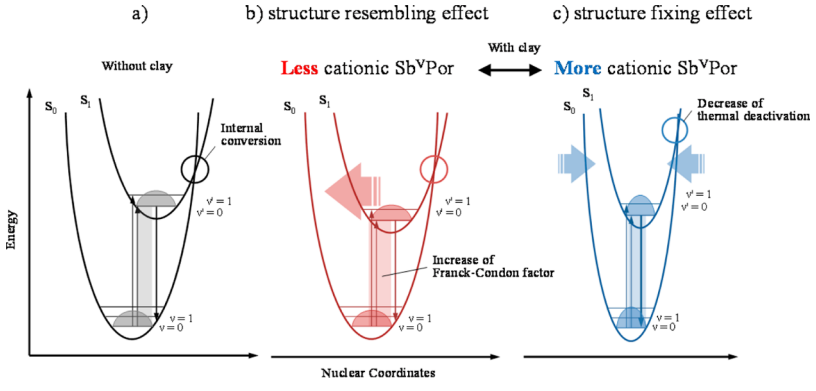

Figure 8. Plausible potential energy curves of the ground and excited states of porphyrins without (a) and with clay (b and c). The structure resembling effect between ground and excited state (effect i) and the structure fixing effect (effect ii) on the clay surface are shown (b and c).

dx.doi.org/10.1021/jp405767s | J. Phys. Chem. A 2013, 117, 7823−7832

Table 4. The Radiative (k_f) and Nonradiative (k_{nr}) Deactivation Rate Constants of $Sb^{V}Por$ with and without Clay in Water[a]

compound	radiative deactivation rate constant (ns^{-1})			nonradiative deactivation rate constant (ns^{-1})		
	k_f^W	k_f^C	k_f^C/k_f^W	k_{nr}^W	k_{nr}^C	k_{nr}^C/k_{nr}^W
$[Sb^{V}(TPP)(OH)_2]Cl$	0.040	0.087	2.2	0.73	1.02	1.4
$[Sb^{V}(DMPyP)(OH)_2]Cl_3$	0.037	0.055	1.5	0.73	0.85	1.2
$[Sb^{V}(TMPyP)(OH)_2]Cl_5$	0.027	0.020	0.75	0.81	0.61	0.75

[a] k^C and k^W are the rate constants of $Sb^{V}Por$ with clay and without clay.

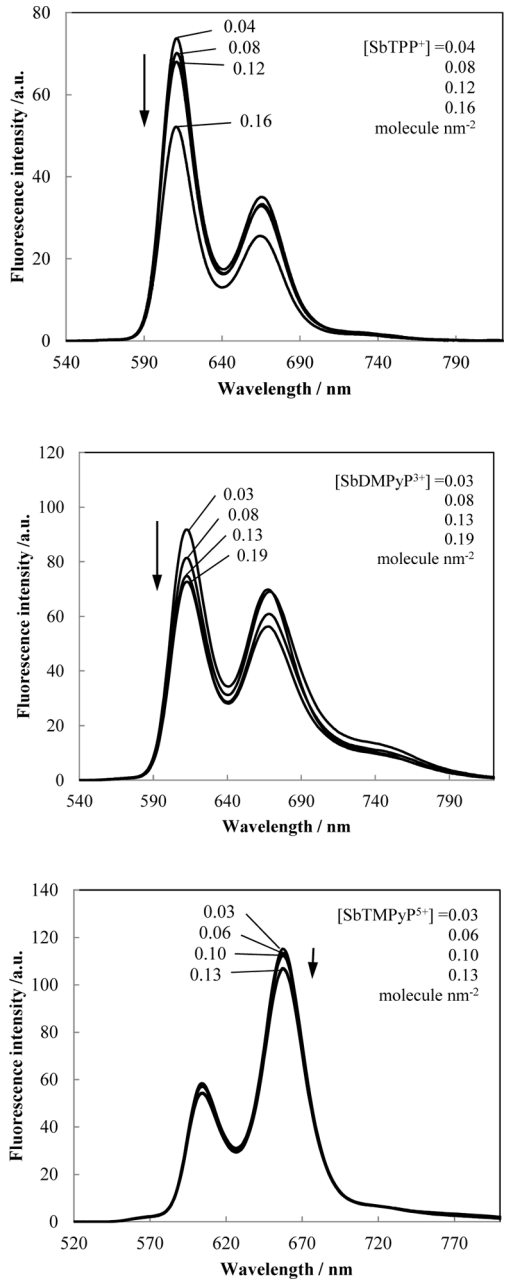

Figure 9. Fluorescence spectra of $Sb^{V}TPP$/saponite complex excited at 431 nm, $Sb^{V}DMPyP$/saponite complex excited at 431 nm, and $Sb^{V}TMPyP$/saponite complex excited at 426 nm in water. [Porphyrin] = 1.0×10^{-7} M.

by changing the concentration of clay. Thus, we can discuss the self-fluorescence quenching by simply comparing the fluorescence intensity. Under these conditions, an aggregation of $Sb^{V}Por$ does not take place.

As the cation number in $Sb^{V}Por$ increased, the fluorescence quenching became less efficient. Especially in the case of $Sb^{V}TMPyP$, the fluorescence quenching was almost not observed. It is expected that the strong adsorption due to the electrostatic interaction between $Sb^{V}TMPyP^{5+}$ and clay should suppress the mobility and collision frequency of molecules, which is essentially needed for an electron transfer reaction. It should be noted that the mobility and collision frequency of molecules should not be effectively suppressed in the case of hydrophobic interaction, since hydrophobic interaction does not work with point to point. The observed suppression of self-fluorescence quenching behavior is valuable to construct an efficient photochemical reaction system.

CONCLUSION

Three types of cationic $Sb^{V}Por$ derivatives were synthesized successfully. The photochemical properties of $Sb^{V}Por$ derivatives with and without clay were investigated. The absorption spectra of $Sb^{V}Por$/clay complexes shifted to longer wavelength due to the flattening of the molecule on the clay surface. The transition probability of the Q-band range of $Sb^{V}Por$ increased, and the relative extinction coefficient of the α Q(0,0) to β Q(0,1) bands increased by the complex formation with clay. For all $Sb^{V}Por$, aggregation behavior was not observed in the clay complexes even at high loading adsorption conditions regardless of the number of cationic parts in $Sb^{V}Por$, judging from the Lambert–Beer plots. This is because of strong electrostatic and hydrophobic interactions between $Sb^{V}Por$ and clay. On the other hand, the fluorescence properties of $Sb^{V}Por$ on the clay surface were different between $Sb^{V}Pors$. The fluorescence quantum yield of less cationic $Sb^{V}Por$ was drastically increased compared to that in water. The increase of fluorescence lifetime was observed in the case of the more cationic $Sb^{V}Por$. These unique fluorescence behaviors would be rationalized by differences of the host–guest interaction including electrostatic and hydrophobic interactions. The effect of complex formation with clay on the potential energy surface of $Sb^{V}Por$ was discussed. For the less cationic $Sb^{V}Por$, increase of its radiative deactivation rate constant was observed on the clay surface due to effect i (structure resembling effect; the most stable structure becomes relatively similar between the ground and excited states) by hydrophobic interaction. For the more cationic $Sb^{V}Por$, decrease of its nonradiative deactivation rate constant was observed on the clay surface due to effect ii (structure fixing effect; sharpened potential energy curves can lead to the increase of activation energy for the internal conversion from excited state to a high vibration level of ground state) by electrostatic interaction. Moreover, the fluorescence quenching of all $Sb^{V}Pors$ was suppressed at even high loading level under nonaggregation conditions. The molecule having a structure such as $Sb^{V}Por$ is important to construct efficient photochemical reaction systems using a clay complex without unexpected fluorescence quenching. In addition, it will be able to control fluorescence properties of the complex by changing

dx.doi.org/10.1021/jp405767s | J. Phys. Chem. A 2013, 117, 7823–7832

the number of cationic parts in the Sb^{V}Por derivatives. These findings are beneficial to construct the efficient photochemical reaction systems in the dye−clay complexes.

■ ASSOCIATED CONTENT

Supporting Information

The synthetic procedures of Sb^{V}Pors and the absorption spectra obtained with s- and p-polarized light for Sb^{V}TPP on the quartz waveguide in water (Figure S1). This material is available free of charge via the Internet at http://pubs.acs.org.

■ AUTHOR INFORMATION

Corresponding Author

*E-mail: takagi-shinsuke@tmu.ac.jp (S.T.). Phone: +81 42 677 2839. Fax: +81 42 677 2838.

Notes

The authors declare no competing financial interest.

■ ACKNOWLEDGMENTS

This work has been partly supported by a Grant-in-Aid for Precursory Research for Embryonic Science and Technology (PRESTO) from the Japan Science and Technology Agency (JST).

■ REFERENCES

(1) Lopez Arbeloa, F.; Martinez, V.; Arbeloa, T.; Lopez Arbeloa, I. Photoresponse and Anisotropy of Rhodamine Dye Intercalated in Ordered Clay Layered Films. *J. Photochem. Photobiol., C* **2007**, *8*, 85−108.

(2) Ras, R.; Umemura, Y.; Johnston, C.; Yamagishi, A.; Schoonheydt, R. Ultrathin Hybrid Films of Clay Minerals. *Phys. Chem. Chem. Phys.* **2007**, *9*, 918−932.

(3) Sato, H.; Hiroe, Y.; Tamura, K.; Yamagishi, A. Orientation Tuning of a Polypyridyl Ru(II) Complex Immobilized on a Clay Surface toward Chiral Discrimination. *J. Phys. Chem. B* **2005**, *109*, 18935−18941.

(4) Takagi, K.; Shichi, T. Clay Minerals as Photochemical Reaction Field. *J. Photochem. Photobiol., C* **2000**, *1*, 113−130.

(5) Thomas, J. K. Physical Aspects of Photochemistry and Radiation Chemistry of Molecules Adsorbed on Silica, γ-Alumina, Zeolites, and Clays. *Chem. Rev.* **1993**, *93*, 301−320.

(6) Bujdak, J. Effect of the Layer Charge of Clay Minerals on Optical Properties of Organic Dyes. A Review. *Appl. Clay Sci.* **2006**, *34*, 58−73.

(7) Takagi, S.; Shimada, T.; Eguchi, M.; Yui, T.; Yoshida, H.; Tryk, D. A.; Inoue, H. High-Density Adsorption of Cationic Porphyrins on Clay Layer Surfaces without Aggregation: The Size-Matching Effect. *Langmuir* **2002**, *18*, 2265−2272.

(8) Bujdak, J.; Komadel, P. Interaction of Methylene Blue with Reduced Charge Montmorillonite. *J. Phys. Chem. B* **1997**, *101*, 9065−9068.

(9) Yui, T.; Kobayashi, Y.; Yamada, Y.; Yano, K.; Fukushima, Y.; Torimoto, T.; Takagi, K. Photoinduced Electron Transfer between the Anionic Porphyrins and Viologens in Titania Nanosheets and Monodisperse Mesoporous Silica Hybrid Films. *ACS Appl. Mater. Interfaces* **2011**, *3*, 931−935.

(10) Thomas, K. J.; Sunoj, R. B.; Chandrasekhar, J.; Ramamurthy, V. Cation-π-Interaction Promoted Aggregation of Aromatic Molecules and Energy Transfer within Y Zeolites. *Langmuir* **2000**, *16*, 4912−4921.

(11) Inagaki, S.; Ohtani, O.; Goto, Y.; Okamoto, K.; Ikai, M.; Yamanaka, K.; Tani, T.; Okada, T. Light Harvesting by a Periodic Mesoporous Organosilica Chromophore. *Angew. Chem., Int. Ed.* **2009**, *48*, 4042−4046.

(12) Fujii, K.; Iyi, N.; Hashizume, H.; Shimomura, S.; Ando, T. Preparation of Integrated Coumarin/Cyanine Systems within an Interlayer of Phyllosilicate and Fluorescence Resonance Energy Transfer. *Chem. Mater.* **2009**, *21*, 1179−1181.

(13) Pushpito, G. K.; Bard, A. Photochemistry of Tris(2,2′-bipyridyl)ruthenium(II) in Colloidal Clay Suspensions. *J. Phys. Chem.* **1984**, *88*, 5519−5526.

(14) Grauer, Z.; Avnir, D.; Yariv, S. Adsorption Characteristics of Rhodamine 6G on Montmorillonite and Laponite, Elucidated from Electronic Absorption and Emission Spectra. *Can. J. Chem.* **1984**, *62*, 1889−1894.

(15) Miyamoto, N.; Kawai, R.; Kuroda, K.; Ogawa, M. Adsorption and Aggregation of a Cationic Cyanine Dye on Layered Clay Minerals. *Appl. Clay Sci.* **2000**, *16*, 161−170.

(16) Bujdak, J.; Iyi, N. Visible Spectroscopy of Cationic Dyes in Dispersions with Reduced-Charge Montmorillonites. *Clays Clay Miner.* **2002**, *50*, 446−454.

(17) Iyi, N.; Sasai, R.; Fujita, T.; Deguchi, T.; Sota, T.; Lopez Arbeloa, F.; Kitamura, K. Orientation and Aggregation of Cationic Laser Dyes in a Fluoromica: Polarized Spectrometry Studies. *Appl. Clay Sci.* **2002**, *22*, 125−136.

(18) Chernia, Z.; Gill, D. Flattening of TMPyP Adsorbed on Laponite. Evidence in Observed and Calculated UV−vis Spectra. *Langmuir* **1999**, *15*, 1625−1633.

(19) Kuykendall, V. G.; Thomas, J. K. Photophysical Investigation of the Degree of Dispersion of Aqueous Colloidal Clay. *Langmuir* **1990**, *6*, 1350−1356.

(20) Kosiur, D. R. Porphyrin Adsorption by Clay Minerals. *Clays Clay Miner.* **1977**, *25*, 365−371.

(21) Cady, S. S.; Pinnavaia, T. J. Porphyrin Intercalation in Mica-type Silicates. *Inorg. Chem.* **1978**, *17*, 1501−1507.

(22) Dias, P. M.; Faria, D. L. A.; Constantino, V. R. L. Clay-Porphyrin Systems: Spectroscopic Evidence of TMPyP Protonation, Non-Planar Distortion and Meso Substituent Rotation. *Clays Clay Miner.* **2005**, *53*, 361−371.

(23) Ogawa, M.; Kuroda, K. Photofunctions of Intercalation Compounds. *Chem. Rev.* **1995**, *95*, 399−438.

(24) Takagi, S.; Shimada, T.; Yui, T.; Inoue, H. High Density Adsorption of Porphyrins onto Clay Layer without Aggregation: Characterization of Smectite-Cationic Porphyrin Complex. *Chem. Lett.* **2001**, *30*, 128−129.

(25) Takagi, S.; Tryk, D. A.; Inoue, H. Photochemical Energy Transfer of Cationic Porphyrin Complexes on Clay Surface. *J. Phys. Chem. B* **2002**, *106*, 5455−5460.

(26) Takagi, S.; Eguchi, M.; Inoue, H. Light Harvesting Energy Transfer and Subsequent Electron Transfer of Cationic Porphyrin Complexes on Clay Surfaces. *Langmuir* **2006**, *22*, 1406−1408.

(27) Eguchi, M.; Takagi, S.; Tachibana, H.; Inoue, H. The 'Size Matching Rule' in Di-, Tri-, and Tetra-Cationic Charged Porphyrin/Synthetic Clay Complexes: Effect of the Inter-Charge Distance and the Number of Charged Sites. *J. Phys. Chem. Solids* **2004**, *65*, 403−407.

(28) Egawa, T.; Watanabe, H.; Fujimura, T.; Ishida, Y.; Yamato, M.; Masui, D.; Shimada, T.; Tachibana, H.; Inoue, H.; Takagi, S. Novel Methodology to Control the Adsorption Structure of Cationic Porphyrins on the Clay Surface Using the "Size-Matching Rule". *Langmuir* **2011**, *27*, 10722−10729.

(29) Ishida, Y.; Masui, D.; Shimada, T.; Tachibana, H.; Inoue, H.; Takagi, S. The Mechanism of the Porphyrin Spectral Shift on Inorganic Nanosheets: The Molecular Flattening Induced by the Strong Host−Guest Interaction due to the "Size-Matching Rule". *J. Phys. Chem. C* **2011**, *116*, 7879−7885.

(30) Kuroda, T.; Fujii, K.; Sakoda, K. Ultrafast Energy Transfer in a Multichromophoric Layered Silicate. *J. Phys. Chem. C* **2010**, *114*, 983−989.

(31) Ogawa, M.; Ide, Y.; Okada, T. Organic-Inorganic Hybrids Based on Ultrathin Oxide Layers - Designed Nanostructures for Molecular Recognition. *Chem.—Asian J.* **2010**, *7*, 1980−1992.

(32) Letaief, S.; Detellier, C. Clay−Polymer Nanocomposite Material from the Delamination of Kaolinite in the Presence of Sodium Polyacrylate. *Langmuir* **2009**, *25*, 10975−10979.

(33) Takagi, S.; Eguchi, M.; Tryk, D, A.; Inoue, H. Porphyrin Photochemistry in Inorganic/Organic Hybrid Materials: Clays, Layered Semiconductors, Nanotubes, and Mesoporous Materials. *J. Photochem. Photobiol., C* **2006**, *7*, 104−126.
(34) Takagi, S.; Shimada, T.; Ishida, Y.; Fujimura, T.; Masui, D.; Tachibana, H.; Eguchi, M.; Inoue, H. Size-Matching Effect on Inorganic Nanosheets: Control of Distance, Alignment, and Orientation of Molecular Adsorption as a Bottom-Up Methodology for Nanomaterials. *Langmuir* **2013**, *29*, 2108−2119.
(35) Tsukamoto, T.; Shimada, T.; Takagi, S. Unique Photochemical Properties of *p*-Substituted Cationic Triphenylbenzene Derivatives on a Clay Layer Surface. *J. Phys. Chem. C* **2013**, *117*, 2774−2779.
(36) Villemure, G.; Detellier, C.; Szabo, A. G. Fluorescence of Clay-Intercalated Methylviologen. *J. Am. Chem. Soc.* **1986**, *108*, 4658−4659.
(37) Villemure, G.; Detellier, C.; Szabo, A. G. Fluorescence of Methylviologen Intercalated into Montmorillonite and Hectorite Aqueous Suspensions. *Langmuir* **1991**, *7*, 1215−1221.
(38) Takagi, S.; Aratake, Y.; Konno, S.; Masui, D.; Shimada, T.; Tachibana, H.; Inoue, H. Effects of Porphyrin Structure on the Complex Formation Behavior with Clay. *Microporous Mesoporous Mater.* **2011**, *141*, 38−42.
(39) Ishida, Y.; Fujimura, T.; Masui, D.; Shimada, T.; Tachibana, H.; Inoue, H.; Takagi, S. What Lowers the Efficiency of an Energy Transfer Reaction between Porphyrin Dyes on Clay Surface? *Clay Sci.* **2012**, *15*, 69−174.
(40) Rillema, D. P.; Nagle, J. K.; Barringer, L. F., Jr.; Meyer, T. J. Redox Properties of Metalloporphyrin Excited States, Lifetimes, and Related Properties of a Series of Para-Substituted Tetraphenylporphine Carbonyl Complexes of Ruthenium(II). *J. Am. Chem. Soc.* **1981**, *103*, 56−62.
(41) Takagi, S.; Suzuki, M.; Shiragami, T.; Inoue, H. Photochemical P-450 Oxygenation of Cyclohexene with Water Sensitized by Dihydroxo-Coordinated (Tetraphenylporphyrinato)antimony(V) Hexafluorophosphate. *J. Am. Chem. Soc.* **1997**, *119*, 8712−8713.
(42) Takagi, S.; Okamoto, T.; Shiragami, T.; Inoue, H. Photochemical Oxygenation of Cyclohexene through Reductive Quenching of Excited Tetraphenylporphyrinatoantimony(V) by Triphenylphosphine. *J. Org. Chem.* **1994**, *59*, 7373−7378.
(43) Takagi, S.; Okamoto, T.; Shiragami, T.; Inoue, H. Photochemical Electron Transfer from Hydroxide Ion to the Excited Triplet State of Tetraphenylporphyrinato-antimony(V) upon Visible Light Irradiation in Aqueous Acetonitrile. *Chem. Lett.* **1993**, 793−796.
(44) Okamoto, T.; Takagi, S.; Shiragami, T.; Inoue, H. Efficient Oxygenation of Alkene through Reductive Quenching of Excited Sb(V)tetraphenylporphyrin by Triphenylphosphine. *Chem. Lett.* **1993**, 687−690.
(45) Lucia, L. A.; Yui, T.; Sasai, R.; Takagi, S.; Takagi, K.; Yoshida, H.; Whitten, D. G.; Inoue, H. Enhanced Aggregation Behavior of Antimony(V) Porphyrins in Polyfluorinated Surfactant/Clay Hybrid Microenvironment. *J. Phys. Chem. B* **2003**, *107*, 3789−3797.
(46) Shiragami, T.; Matsumoto, J.; Inoue, H.; Yasuda, M. Antimony Porphyrin Complexes as Visible-Light Driven Photocatalyst. *J. Photochem. Photobiol., C* **2005**, *6*, 227−248.
(47) Shiragami, T.; Shimizu, Y.; Hinoue, K.; Fueta, Y.; Nobuhara, K.; Akazaki, I.; Yasuda, M. Silica Gel-Supported Porphyrinatoantimony-(V) Complex Acting as Visible-Light Driven Photocatalyst for Dechlorination of Chlorophenols in Aqueous Solution. *J. Photochem. Photobiol., A* **2003**, *156*, 115−119.
(48) Inoue, I.; Funyu, S.; Shimada, Y.; Takagi, S. Artificial Photosynthesis via Two-Electron Conversion: Photochemical Oxygenation Sensitized by Ruthenium Porphyrins with Water as Both Electron and Oxygen Donor. *Pure Appl. Chem.* **2005**, *77*, 1019−1033.
(49) Funyu, S.; Isobe, T.; Takagi, S.; Tryk, D. A.; Inoue, H. Highly Efficient and Selective Epoxidation of Alkenes by Photochemical Oxygenation Sensitized by a Ruthenium(II) Porphyrin with Water as Both Electron and Oxygen Donor. *J. Am. Chem. Soc.* **2003**, *125*, 5734−5740.
(50) Shiragami, T.; Andou, Y.; Hamasuna, Y.; Yamaguchi, F.; Shima, K.; Yasuda, M. Effects of an Axial Ligand on the Reduction Potential, Proton Dissociation, and Fluorescence Quantum Yield of Hydroxo-(porphyrinato)antimony(V) Complexes. *Bull. Chem. Soc. Jpn.* **2002**, *75*, 1577−1582.
(51) Shiragami, T.; Nabeshima, K.; Nakashima, S.; Matsumoto, J.; Takagi, S.; Inoue, H.; Yasuda, M. Effects of Axial Ligands on the Formation of a Layered Structure in Mono- and Di-Cationic Charged Tetraphenylporphyrinatoantimony(V)/Synthetic Clay Composites. *Bull. Chem. Soc. Jpn.* **2005**, *78*, 2251−2258.
(52) Shiragami, T.; Nabeshima, K.; Yasuda, M.; Inoue, H. Roles of Axial Ligands on Intercalation of Cationic Metalloporphyrin into Smectite Clay Layers. *Chem. Lett.* **2003**, *2*, 148−149.
(53) Shiragami, T.; Nabeshima, K.; Matsumoto, J.; Yasuda, M.; Inoue, H. Non-Aggregated Intercalation of Dicationic Tetraphenylporphyrinatoantimony(V) Complexes into Smectite Clay Layers. *Chem. Lett.* **2003**, *6*, 484−485.
(54) Eguchi, M.; Takagi, S.; Inoue, H. The Orientation Control of Dicationic Porphyrins on Clay Surface by Solvent Polarity. *Chem. Lett.* **2006**, *35*, 14−15.
(55) Eguchi, M.; Tachibana, H.; Takagi, S.; Tryk, D. A.; Inoue, H. Dichlonic Mesurements on Dicationic and Tetracationic Porphyrins on Clay Surfaces with Visible-Light-Attenuated Total Reflectance. *Bull. Chem. Soc. Jpn.* **2007**, *80*, 1350−1356.
(56) De Paoli, M. V.; De Paoli, H. S.; Borissevitch, E. I.; Tedesco, C. A.; Inoue, H. Fluorescence Lifetime and Quantum Yield of $TMPyPH_2$ Associated with Micelles and DNA. *J. Alloys Compd.* **2002**, *344*, 27−31.